Supporting Information

SnO_2 Nanowire/MoS_2 Nanosheet Composite Gas Sensor in Self-Heating Mode for Selective and ppb-Level Detection of NO_2 Gas

Jin-Young Kim[1], Ali Mirzaei[2,*], Jae-Hun Kim[1,*]

[1]Department of Materials Science and Engineering, Inha University, Incheon 22212, Republic of Korea

[2]Department of Materials Science and Engineering, Shiraz University of Technology, Shiraz, Iran

*Corresponding Authors

E-mail address: mirzaei@sutech.ac.ir (A. Mirzaei), jaehun@inha.ac.kr (J.-H. Kim).

Text S1:

The limit of detection limit (LOD) is an important indicator that reflects the sensing performance. The lower LOD is defined as the minimum concentration at which the response differs significantly from the noise signal. Sensor noise can be calculated by changing the relative response of the sensor over the baseline. Before exposure to NO_2, we took the average value of 20 consecutive data points, and then the root mean square error (RMS) was calculated as follows [S1].

$$\mathrm{RMS}_{noise} = \sqrt{\frac{S^2}{N}} \quad (1)$$

Where N=20 is the number of data points. Then, DOL was calculated as follows [S1]:

$$\mathrm{DOL} = 3\frac{RMS_{noise}}{Slope} \quad (2)$$

Since RMS was equal to 0.0034 and slope of calibration curve was 0.568, DOL was calculated to be $3 \times 0.0034/0.568 = 0.0179$ ppm (17.9 ppb). The theoretical calculation results showed negligible differences of about 3 ppb with LOD obtained experimentally.

[S1] Choi, M.S., Bang, J.H., Mirzaei, A., Oum, W., Na, H.G., Jin, C., Kim, S.S. and Kim, H.W., 2019. Promotional effects of ZnO-branching and Au-functionalization on the surface of SnO_2 nanowires for NO_2 sensing. *Journal of Alloys and Compounds*, *786*, pp.27-39.

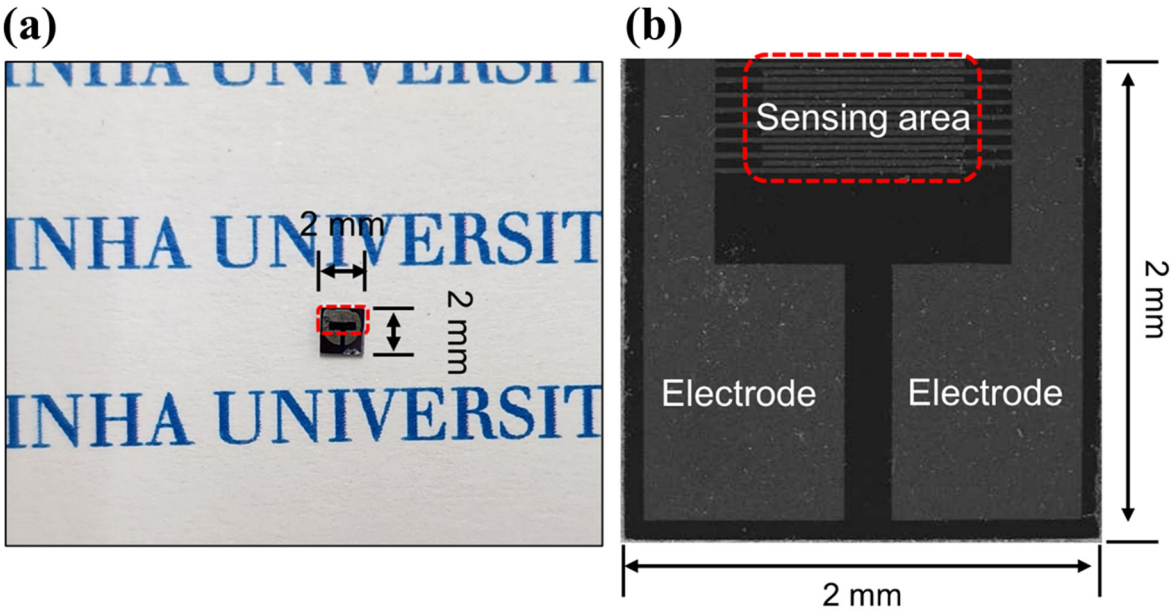

Figure S1. (a,b) Digital images of fabricated sensor.

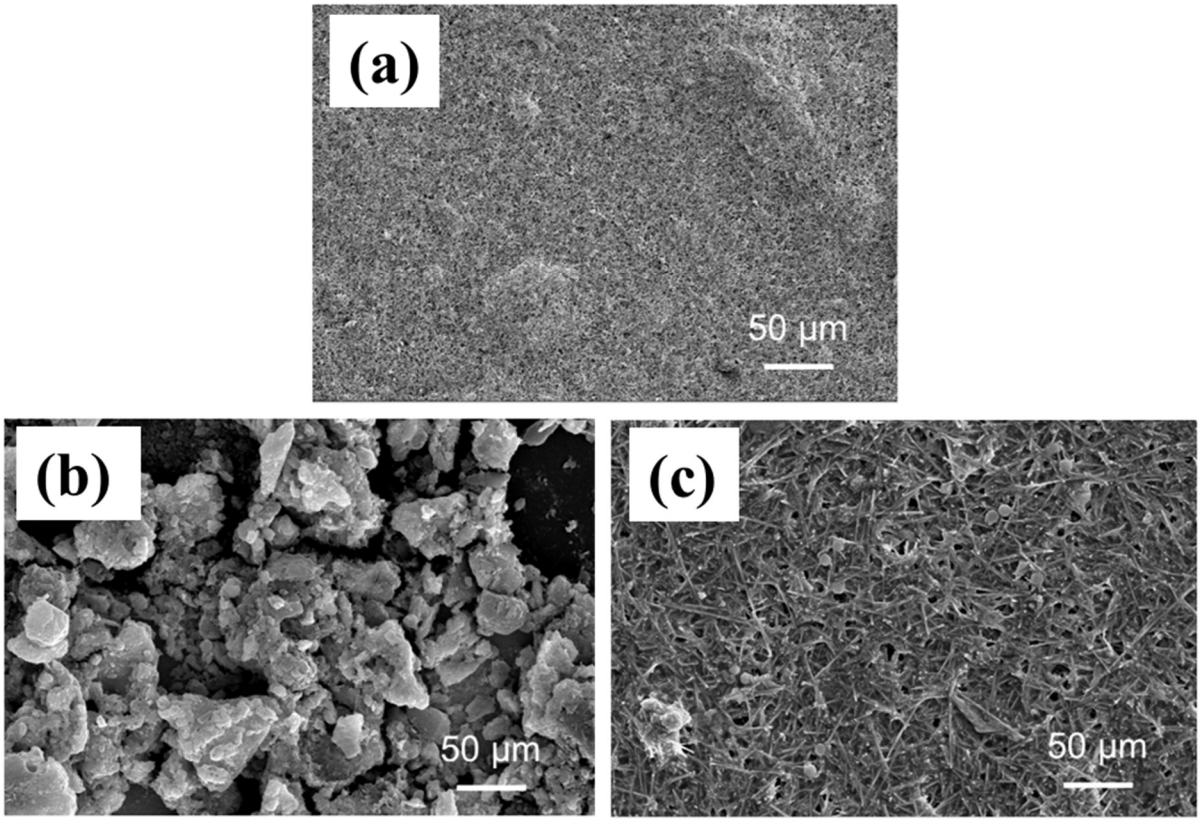

Figure S2. SEM images of (a) SnO_2 NW, (b) MoS_2 NSs, and (c) SM-20 nanocomposite.

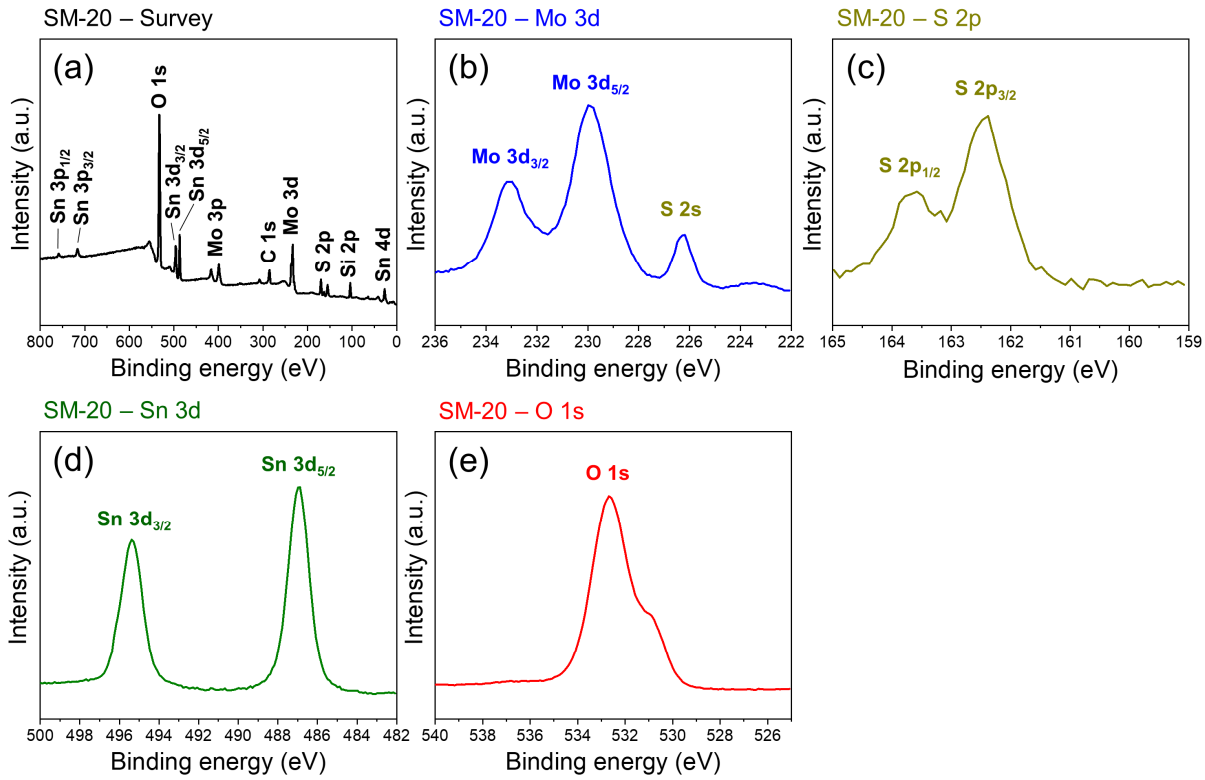

Figure S3. (a) XPS survey of SM-20 composite. XPS core-level regions of (b) Mo 3d, (c) S 2p, (d) Sn 3d, and (e) O 1s.

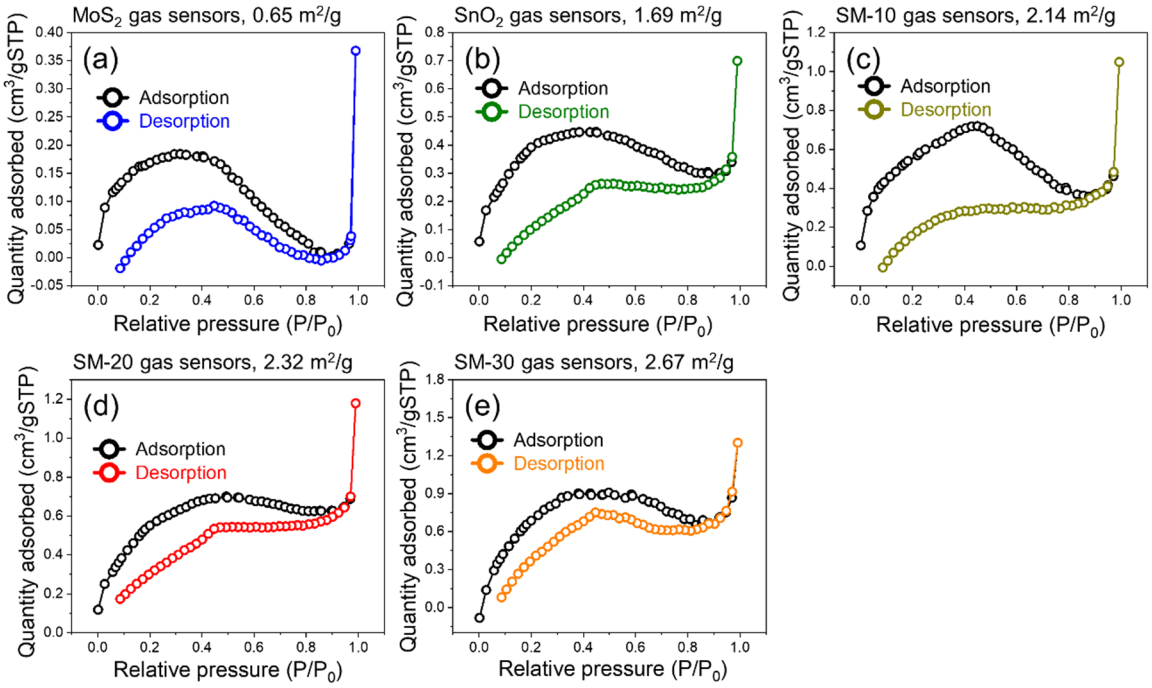

Figure S4. N_2 adsorption-desorption isotherms of (a) MoS_2 NSs, (b) SnO_2 NWs, (c) SM-10, (d) SM-20, and (e) SM-30 nanocomposite.

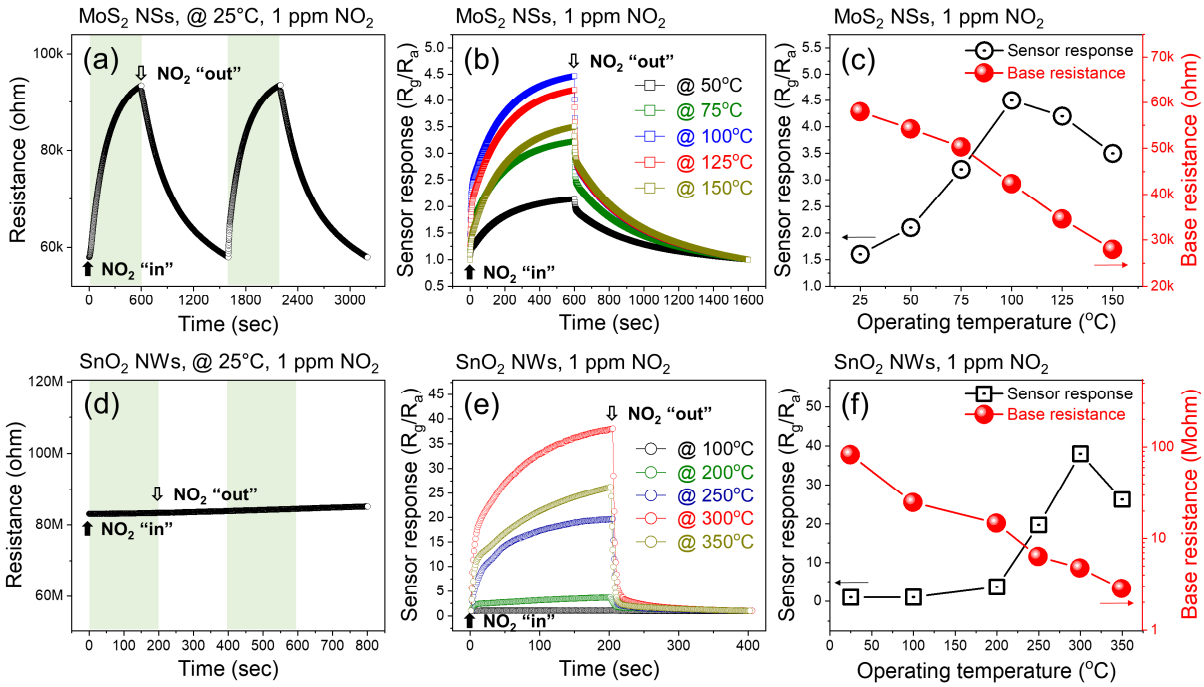

Figure S5. Dynamic resistance and dynamic response plots of pristine MoS_2 NS gas sensor to 1 ppm NO_2 at (a) 25°C and (b) different temperature (50-150°C) under 1 V applied voltage. (c) Corresponding NO_2 gas response and baseline resistance versus operating temperature. Dynamic resistance plots of pristine SnO_2 NW gas sensors to 1 ppm NO_2 at (d) 25°C and (e) different temperature (50-350°C) under 1 V applied voltage. (f) Corresponding NO_2 gas response and baseline resistance versus operating temperature.

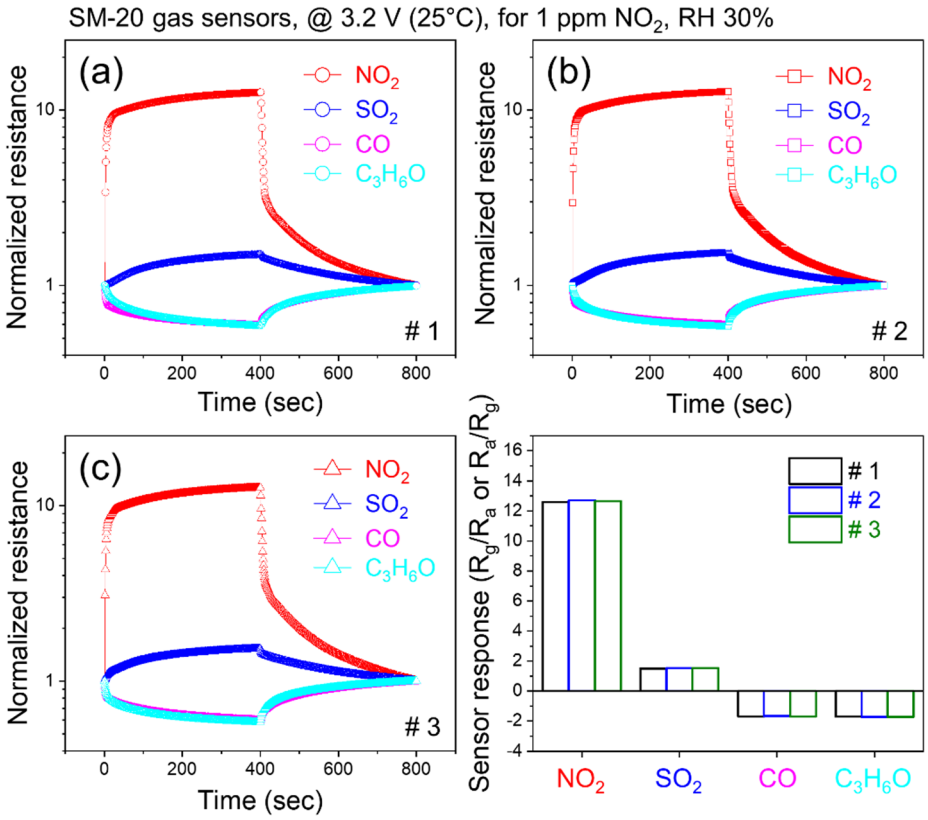

Figure S6. Reproducibility tests of three SM-20 gas sensors prepared under the same conditions. Sensing performance of SM-20 gas sensor (a) number 1 (b) munber 2 and (c) number 3 (a) to low concentrations of various gases at fixed 3.2 V. (d) Corresponding selectivity histograms of three gas sensors.

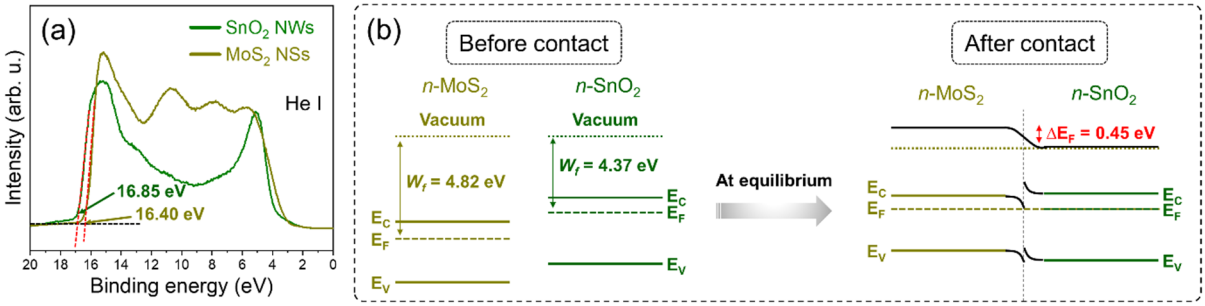

Figure S7. (a) UPS spectra and energy cut-off values of MoS_2 NSs and SnO_2 NWs. (b) Energy band levels of MoS_2 NSs and SnO_2 NWs before and after intimate contact.

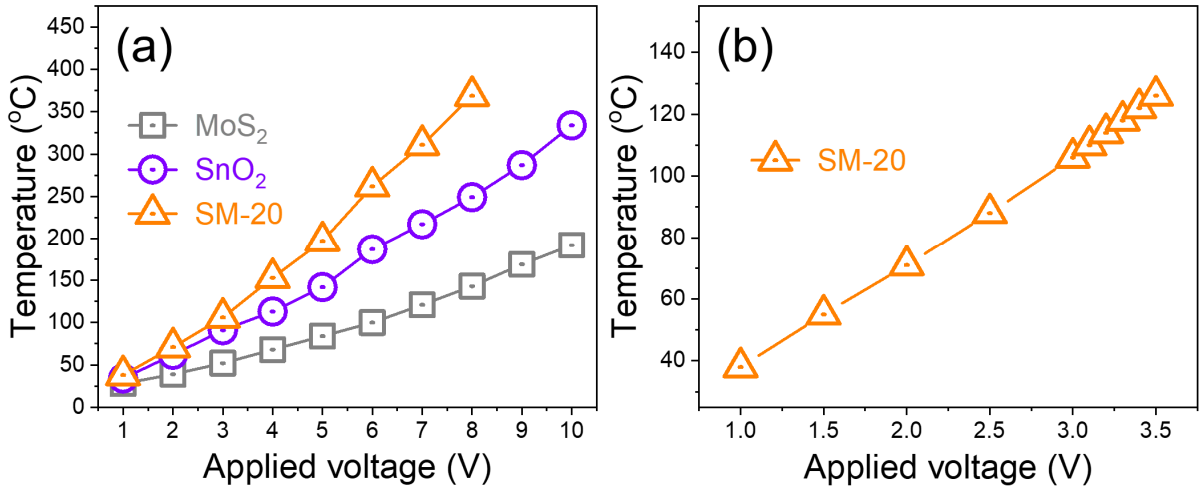

Figure S8. (a) Sensor temperature versus applied voltage for different gas sensors. (b) Temperature of SM-20 gas sensor versus applied voltage in the range of 1 to 3.5 V.